Journal of Photochemistry and Photobiology A: Chemistry 329 (2016) 203–212

Contents lists available at ScienceDirect

Journal of Photochemistry and Photobiology A: Chemistry

journal homepage: www.elsevier.com/locate/jphotochem

Effect of neutral salts on the excited state proton transfer in the fluorescent probe anchored to the uncharged micelles

Andrzej Jankowski[a], Adam Jankowski[b], Alicja Kluczyk[a], Anna Szemik-Hojniak[a,*]

[a] Faculty of Chemistry, University of Wroclaw, Joliot-Curie 14 st, 50-383 Wroclaw, Poland
[b] Medical University of Wrocław. Clinic of Immunology and Rheumatology, the J. Gromkowski Hospital, ul. Koszarowa 5, 51-149 Wrocław, Poland

ARTICLE INFO

Article history:
Received 13 April 2016
Accepted 24 June 2016
Available online 29 June 2016

Keywords:
Fluorescence
2-Naphthol derivative bound to micelles
Excited state proton transfer
Nonionic micelles
Salt impact on micelles

ABSTRACT

We study the salt effect on the excited state proton transfer (ESPT) in the fluorescent probe of 2-hydroxynaphthalene (dodecylo)-6-sulphonamide (NSDA) anchored on the nonionic Brij35 micelles. The results of spectrofluorimetric, electrophoretic and equilibrium dialysis measurements, allowed us to explain the variations in the ESPT rate constants in the presence of different neutral salts (NaCl, KCl, KSCN, NH_4SCN) as resulting from anion accumulation at the particle surface. Similarly to electric double layer in the charged micelles, an ionic layer system is also formed around the nonionic micelles. The dimensions of anionic and cationic layers as well as those of the whole ionic envelope around the nonionic particles are estimated. Furthermore, the electric potential generated within the ionic layer system and acting on the proton dissociating from the probe is determined and interpreted. Different impact of Cl^- and SCN^- ions on photophysical parameters of the targeted system have been explained through a synergy effect between hydrophobicity and polarizability of anions adsorbing on the nonionic micelle surface.Taking into account the existing analogy between micelles and living cells, we can assume that these results will contribute to a better understanding of salt effect in such important biological phenomena as the cell adhesion to surfaces, thermal denaturation of proteins and the aggregation of erythrocytes.

1. Introduction

Recently, the relations between ESPT (excited state proton transfer) rate constants in NSDA [2-hydroxy naphthalene (dodecylo)-6-sulphonamide] bound to nonionic Brij35 micelles along with their surface potential and the ionic gradients in the created electric double layer (EDL) were analyzed [1]. Furthermore, advantages and benefits of using NSDA as a new proton-transfer fluorescent probe were also presented [1].

In general, the studies of ESPT in the probe bound to micelles can supply important information on ion distribution around the colloidal particles. They also allow for a deeper recognition of multiphase and biological systems [2–5]. Recently appeared some very interesting papers [5g–5i] dealing with the ESPT of probes bound to the nonionic micelles.

Regarding the stabilizing electrolyte effect, it is only hypothesized [5a] that anions may preferentially be accumulated at an uncharged particle surface, forming in this way a layer that maintains all colloidal particles in the solution.

In the present study, applying the above mentioned approach, we were able to trace the formation of the ionic layer system in the presence of different salts. The obtained results enabled us to estimate both the dimensions of the first ionic layer as well as the whole ionic envelope surrounding the nonionic Brij35 micelles. Expecting a different influence of anion polarizability on the micelles properties [4a,6], several salts (NaCl, KCl, KSCN and NH_4SCN) varying in polarizability and hydration energy were chosen for experiment. On the basis of the obtained results, the modified model that explains the influence of applied ions on the physico–chemical properties of micelles, has been suggested.

2. Materials and methods

2.1. Synthesis of the fluorescent probe and its binding to micelles

The 2-hydroxynaphthalene(dodecylo)-6-sulphonamide (NSDA, Fig. 1a) was prepared according to the method used in synthesis of sulphonamides described in Ref. [7] (see also Ref. [1]).

* Corresponding author.
E-mail addresses: andrzej.jankowski@chem.uni.wroc.pl (A. Jankowski), jankaw@prop.am.wroc.pl (A. Jankowski), alicja.kluczyk@chem.uni.wroc.pl (A. Kluczyk), anna.szemik@chem.uni.wroc.pl (A. Szemik-Hojniak).

http://dx.doi.org/10.1016/j.jphotochem.2016.06.028
1010-6030/

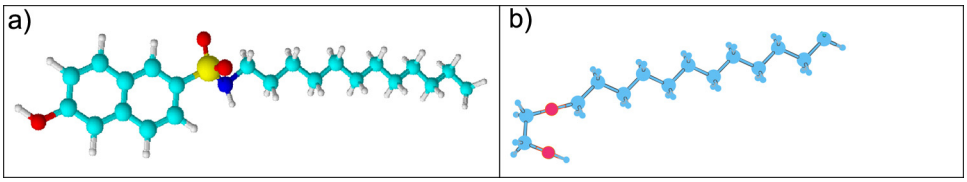

Fig. 1. The molecular structure of NSDA (1a). The molecular structure of the Brij35 monomer (1b): Carbon atoms—light blue, oxygen—red, hydrogen—grey, sulfur—yellow, nitrogen—dark blue. (For interpretation of the references to colour in this figure legend, the reader is referred to the web version of this article.)

The detergent used for the formation of the uncharged micelles: polyoxy-ethyleneglycol dodecyl ether (Brij35, Fig. 1b), was obtained from Calbiochem.

The appropriate amounts of NSDA, surfactant (S) and the salt were weighted, in a way allowing us to obtain a final (S) concentration higher than the critical micelle concentration (CMC). NSDA concentration values, near to 5.0×10^{-5} M, showing absorbance at the sample excitation wavelength of 5.0×10^{-2}–1.0×10^{-1} [$M^{-1}\,cm^{-1}$] and the proportion of NSDA to micelles near to 1:1 was used. The concentration of micelles was calculated similarly as in Ref. [8] taking into account that 40 molecules of Brij35 are included into one micelle [9]. Both samples (NSDA and S) were dissolved in methanol (2.5 cm^3, spectral grade) and the solution of NSDA was added dropwise to that of (S) while stirring. Then, the mixture was dried and the residual material was dissolved in 5 cm^3 of hot (50 °C, conductivity 9.0×10^{-2} μS) water by stirring during 30 min. After cooling the sample to the room temperature, the salt was added to obtain its required concentration. The resulting solution was clear and transparent and showed the fluorescence characteristic of 2-naphthol derivatives.

2.2. Determination of the ESPT rate constants by spectrofluorimetric methods

The fluorescence spectra were recorded by means of M-31 spectrofluorimeter (Optel, Poland) as described elsewhere [10]. In the presence of salts, the maxima of excitation fluorescence spectra have shifted merely about 1–2 nm in direction of the longer wavelengths (red shift) with respect to excitation spectra in the salt free solution.

The fluorescence lifetimes were measured by means of the combined Steady State and Time-Resolved Spectrofluorimeter (FLS920) of Edinburg Instruments.

The ESPT process [11,12] can be represented by the scheme in Fig. 2

The values of the deprotonation (k_{DP}) and the protonation rate constant (k_{PP}, Fig. 2) were determined from Formula (1) [11a] and Formula (2) [12a–c].

$$k_{DP} = [(\Phi_N'/\Phi_0')(\tau_0'/\tau_N')]/\tau_N \quad (1)$$

$$(\Phi/\Phi_0)/(\Phi'/\Phi_0') = (k_{DP}\,\tau_0)^{-1} + \{(k_{PP}^{app}\,\tau_0'/k_{DP}\,\tau_0)\}\,f\,[H_3O^+] \quad (2)$$

where: Φ_N, Φ_0—means the fluorescence quantum yield of the ROH* form at the neutral pH in the plateau region (where the ESPT takes place, see Fig. 5S) and at the pH lower than the excited state pK_a^* value (where no ESPT reaction is observed), respectively; Φ_N', Φ_0' is the fluorescence quantum yield of the RO^{-*} form at the neutral pH and at pH >> pK_a where the ionized form is directly excited. It should be noticed that the pK_a of NSDA in the ground state is near to 10 while the excited state pK_a^* diminishes to 0. The Φ and Φ'—are the fluorescence quantum yield of ROH* and RO^{-*} form, respectively, at a given pH; the τ_0, τ_N—are the excited state lifetimes of the protonated (ROH*) form at pH << pK_a^* and at neutral pH, respectively, while the τ_0', τ_N' are the excited state lifetimes of the deprotonated (RO^{-*}) species at pH >> pK_a and at the neutral pH value, respectively. One should add that in the acidic pH, the decay of excited fluorophore follows the monoexponential function while in the vicinity of neutral pH, we observed the bi-exponential decay. The Chi^2 was in the region 0.8–1.5.

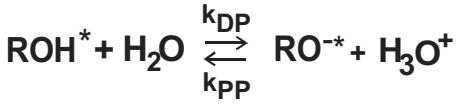

Fig. 2. Schematic illustration of the ESPT reaction in water; R—means NSDA nonpolar core (asterisk designates that the probe occurs in its first excited state). The changes of acidity were achieved by addition of 0.001–1 M of HCl.

The proton kinetic activity coefficient "f" in Eq. (2) was determined from Eq. (2a) given below (see Refs. [12a,13]).

$$\log f = [(1.02J^{0.5})/(1 + 2\,J^{0.5})], \quad (2a)$$

where:- J is the ionic strength ($J = 0.5 \sum z_i C_i$) and z_i, c_i are the valence and concentration of all ions present in the solution. From the plot of the ordinate of Eq. (2) *versus* the f x [H_3O^+] and using the k_{DP} value calculated from Eq. (1), the ($k_{PP}t_0'$)/($k_{DP}t_0$) ratio and then the apparent protonation rate constant (k_{PP}^{app}) is obtained. The k_{PP} value-is determined by taking into account the rate constant of the quenching process by H^+ ions (k_{H^+}), $k_{PP} = k_{PP}^{app} - k_{H^+}$. The k_{H^+} value was obtained from the plot of $(F_\Sigma^0 - F_\Sigma)/F_\Sigma$ as a function of [H_3O^+] where F_Σ^0, F_Σ is the fluorescence intensity at the neutral pH and at a given pH value while the subscript Σ- means that the sum of the fluorescence intensities of the ROH* and RO^{-*} bands is taken into account. For the more detailed presentation of the k_{PP} determination procedure see Ref [1] and Fig. 3S.

To estimate the role of ESPT in the presence of other excited state processes competing with ESPT such as the quenching by SCN^- ($\mathbf{k^{SCN-}}$), or by Cl^- ($\mathbf{k^{Cl}}$) ions, the method based on the determination of the isoemissive wavelength ($\boldsymbol{\lambda_{ie}}$) was applied. The $\boldsymbol{\lambda_{ie}}$ appears usually using the spectrofluorimetric titrations of compounds undergoing ESPT when a factor affecting ESPT (eg. mineral acid or neutral salt) is added to the solution [1,14] (see Figs. 1S and 5S). The λ_{ie} can be conveniently determined at a low quencher concentration when the quenching effect is negligible. The emission intensities obtained at the higher quencher concentration (Cq) were multiplicated by the $W = F^0{}_{\lambda ie}/F^{Cq}{}_{\lambda ie}$ coefficient, where: $F^0{}_{\lambda ie}$ is the fluorescence intensity at λ_{ie} wavelength in the absence of the quencher whereas the $F^{Cq}{}_{\lambda ie}$, is the intensity at the λ_{ie} for a given Cq value. Further details of the ESPT rate constants (k_{DP}, k_{PP}) and equilibrium constants ($K_a^* = k_{DP}/k_{PP}$) determinations are given in Ref. [1,10].

The ESPT reaction presented simply by the scheme of Fig. 2, can be also depicted as a two – step process (Fig. 3).

The ESPT rate constants (k_{dpi}, k_{ppe}) and the rate constants ratios (k_{NR}/k_{dpe}, k_{NR}/k_{ppi}, k_{ppi}/k_{dpe}) were calculated by the methods given in Ref. [[11a], see also Appendix A where the methods for k_{NR}, k_{dpe} and k_{ppe} determination are given].

The inner sphere proton transfer rate constants (k_{dpi}, k_{ppi}) reflect the proton movement along the OH bond during the ESPT process while those of the outer sphere (k_{dpe}, k_{ppe}) are associated